 DOI: 10.1002/masy.201300123

High-Temperature Viscoelastic Relaxation in All-Cellulose Composites

Benoît J.C. Duchemin,*[1] *Mark P. Staiger*,[2] *Roger H. Newman*[3]

Summary: All-cellulose composites were prepared across a range of different crystallinities in order to examine relationships between phase composition and viscoelastic behaviour in the temperature range of 270 °C to 340 °C corresponding to the α_1 mechanical relaxation. Composite films were prepared by partial dissolution of microcrystalline cellulose in a LiCl/*N,N*-dimethylacetamide (LiCl/DMAc) solvent system using the film casting technique. Dynamic mechanical analysis showed two contributions to α_1 relaxation, with tan δ maxima at 303 ± 2 °C and at approximately 325 °C. The height of the maximum or shoulder at 303 ± 2 °C decreased with increasing crystallinity, and was therefore assigned to molecular motion associated with chemical decomposition in non-crystalline domains. The maximum at 325 °C was assigned to chemical decomposition in chains associated with the surfaces of crystalline domains. Composites with high crystallinity showed best retention of the dynamic storage modulus when tested at 300 °C.

Keywords: all-cellulose composites; crystal structures; polysaccharides; viscoelastic properties

Introduction

Much research has focused on using cellulose fibres to reinforce polymer matrices, since cellulose is the most abundant polymer produced in nature and has high mechanical properties and thermal stability.[1,2] Due to a well-ordered network of intermolecular hydrogen bonds, the linear cellulose chains can align and form sheets that can in turn stack longitudinally and form crystallites.[2,3] As a result, the cellulosic crystalline assembly exhibits a high stiffness (137–138 GPa) that outperforms many of the most common man-made polymers.[1,4] Recently, biocomposites have been investigated in which the reinforcement and matrix are both based on pure cellulose. Nishino et al. named these materials all-cellulose composites.[5] They were intended to avoid the chemical incompatibilities of hydrophilic cellulose and hydrophobic synthetic polymers.[5–9] In addition, all-cellulose composites have a high thermal stability and can retain a dynamic storage modulus as high as 20 GPa when heated to 300°C.[5] We sought to identify factors that influence this thermal stability, so that we might better design composites for high-temperature applications.

The glass transition of polymers is defined as the temperature at which an amorphous polymers goes from the glass to the rubber phase. The glass transition of cellulose is a second order transition, characterized by a heat capacity and thermal expansion increase, and decrease in elastic modulus.[10–12] As the polymer undergoes the glass transition, an increase of its free volume allows the polymer chains greater freedom of motion. The determination of the glass transition for native celluloses is a difficult task as the results

[1] Laboratoire Ondes et Milieux Complexes, UMR 6294, CNRS-Université du Havre, 53 rue Prony BP540, 76058 Le Havre, France
E-mail: benoit.duchemin@univ-lehavre.fr
[2] Department of Mechanical Engineering, University of Canterbury, Private Bag 4800, Christchurch, New Zealand
[3] Scion, Private Bag 3020 Rotorua Mail Centre, Rotorua 3046, New Zealand

will be largely dependant on the moisture content, structure and crystallinity of the materials.[11,12] Differential scanning calorimetry (DSC) is a tool that is commonly used to detect glass transitions of polymers. However, DSC is relatively insensitive to the small variations in heat capacity associated with the glass transitions in cellulose.[11,13] Dynamic mechanical analysis (DMA) has been used with greater success in the past on regenerated cellulose. DMA is able to reveal three separate glass transitions, labelled α_1, α_2 and α_3.[14] The α_3 transition, near 30 °C, was assigned to cooperative motions of cellulose chains and water molecules in non-crystalline regions. The transitions labelled α_2 (near 140 °C) and α_1 (near 300 °C) were assigned to micro-Brownian motions of polymer segments in non-crystalline regions. The α_1 transition is of special interest in this work as it occurs close to the temperature at which cellulose decomposes. Other authors have contributed to characterisation of the α transitions.[15–18]

Hydrogen bonding governs the viscoelastic behaviour of cellulose.[18] Hydrogen bonding in non-crystalline cellulose involves mostly C-2 and C-3 hydroxyl groups.[19] Hydrogen bonding in the highly ordered crystalline states involves additional participation of the C-6 hydroxymethyl group.[20–22] As a result of the differences in hydrogen bonding, lower intermolecular cohesive forces are experienced by the non-crystalline phase. It was suggested that the multiple α transitions might reflect distinct segmental environments in non-crystalline cellulose, with distinct densities of hydrogen bonding.[14] In the case of the α_1 transition, it was also suggested that the segments might be partly immobilised by association with crystalline domains.[14]

In the present work, DMA was used to characterise α_1 relaxation for all-cellulose composites prepared with different ratios of crystalline particles to non-crystalline matrix. This ratio was controlled by varying two parameters in the preparation of all-cellulose composites: (i) the cellulose concentration c in the cellulose-LiCl/DMAc mixture and (ii) the period of time t that the cellulose was left in contact with LiCl/DMAc.

Experimental Part

Preparation of Cellulose and Solvent

Microcrystalline cellulose powder (MCC, Avicel®, Merck Ltd., Germany) was used as a starting material with particle sizes in the range of 20–160 μm. Before use, the MCC was "activated" to aid cellulose dissolution as described previously.[23] Briefly, activation involves successive 24 h long solvent exchange steps with water, acetone and *N,N*-dimethylacetamide (DMAc), followed by drying. A DP of 163 was measured after activation using the method of Bianchi et al.[24]

Reagent-grade lithium chloride (99% purity, Unilab) and *N,N*-dimethylacetamide (DMAc, Merck, Germany) were used as the solvent system for cellulose. A solution of 8.0% (by total weight) LiCl in DMAc was prepared by mixing LiCl (dried in a vacuum oven at 180°C overnight) and DMAc (dried over 4 Å molecular sieve prior to use) in a 200 ml Schott bottle that was immediately sealed to minimise moisture uptake. The mixture was mechanically stirred for 24 h to completely dissolve the LiCl.

Preparation of All-Cellulose Composites

Two phase cellulose materials were prepared by partial dissolution of MCC. Activated MCC was combined with LiCl/DMAc to give cellulose concentrations of $c = 5\%$, 10%, 15% and 20%, where c is expressed as % of the total weight of cellulose, LiCl and DMAc. The solution was homogenised by stirring at 20°C for 2 min. The solution was then poured into a Petri dish and stored under a dry atmosphere at 20°C for dissolution times (t) of 1 and 8 h. The precipitation of the dissolved cellulose was initiated with light spraying of water onto the surface of the solution in order to fix the shape of the final sample. The partially precipitated solution was then

carefully immersed in tap water for 48 h at 20°C. The water was changed at least every 24 h. Residual LiCl and DMAc were completely removed by further thorough rinsing of the specimen with water. The resulting hydrogels were then lightly pressed between paper towelling to remove excess water. Finally, specimens were dried in a vacuum bag (16–24 kPa) at 60°C for 48 h.

Materials Characterization

Wide angle X-ray diffraction (WAXD) was carried out using a Philips PW1729 diffractometer using Cu K_α radiation ($\lambda = 0.15418$ nm). A crystallinity index (*CrI*) was determined as defined by Segal et al.:[25]

$$CrI = 100(I - I')/I \quad (1)$$

where I is the maxima of the diffraction peak corresponding to the reflection of the (200) planes in the range $2\theta = 21°$ to 23°, and I' is the height measured at $2\theta = 18°$, i.e., the position of a broad peak in a diffractogram of pure non-crystalline cellulose.

Dynamic mechanical analysis (DMA) was performed in tension mode with a Perkin Elmer Diamond DMA under a constant flow (400 ml/min) of dry nitrogen to avoid thermal oxidation. The tests were performed in load control. DMA specimens were prepared as thin strips 7–8 mm in width, 0.1–0.4 mm in thickness and 20 mm in gauge length. Specimens were dried under vacuum (24 kPa) at 60 °C for 12 h and 100 °C for a further 4 h and then stored under vacuum. Specimens were then conditioned at 23 °C and 55% R.H. for 1 week before testing. A heating rate of 2°C/min was used and a dynamic strain of 0.05% was imposed at a frequency of 1 Hz. At least two specimens were tested for each all-cellulose composite. The exact determination of the peak position was made difficult by the high energy of high temperature relaxations, partial peak overlapping and relatively low scan resolution. Hence, multifrequency data could not be exploited.

Results and Discussion

Phase Compositions

The phase composition of the composites in this work were described in detail elsewhere.[23,26] Briefly, these composites consist of a continuous paracrystalline cellulose matrix in which undissolved cellulose I crystallites are embedded. The paracrystalline matrix is distinct from cellulose II and corresponds to a poorly crystalline form of cellulose I where the ordered regions would be sufficiently small such that all the polymer chains are exposed to the surface.[23] In general, the amount of remaining undissolved cellulose increased with the initial concentration of cellulose in the solvent. This increase is reflected with increases in the values of *CrI*. Values of *CrI* have also been reported elsewhere for all of the composites used in this work.[23,26] It was reported by Conio et al. that cellulose will not dissolve completely if $c > 11\%$ in 8 wt.% LiCl/DMAc.[27] Thus, a portion of the MCC was expected to be insoluble for $c \geq 15\%$, and that expectation was confirmed by relatively high values of *CrI* for composites prepared with $c \geq 15\%$. The value of *CrI* increased from approximately 40% to 70% when the value of c was increased from 5% to 20%, but was not greatly influenced by increasing t from 1 h to 8 h.

Viscoelastic Relaxation

A typical DMA trace (Fig. 1) showed all three α transitions, but the α_3 and α_2 transitions were relatively weak. The remainder of this work is focused on the α_1 transition.

The α_1 transition contributed peaks at temperatures in the range 303 ± 2 °C regardless of cellulose crystallinity (Figs. 2 and 3). In some cases, the traces showed a shoulder on the high temperature side. This is labelled $\alpha_{1,1}$ in Fig. 2 and 3, in order to distinguish it from the main peak which is labelled $\alpha_{1,2}$. The $\alpha_{1,1}$ peak is most clearly seen at 325 °C in traces obtained for the two composites with highest crystallinity ($c = 20\%$). Charring resulted in disintegration of some of the specimens as the DMA

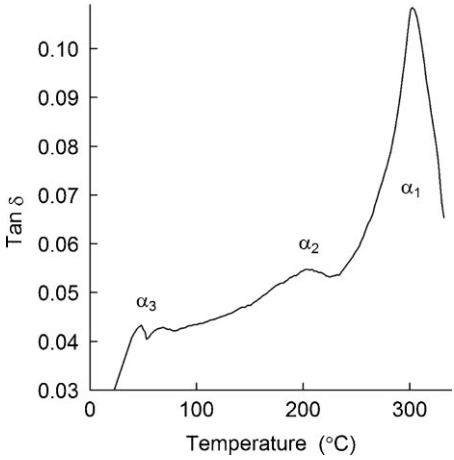

Figure 1.
A typical DMA trace from room temperature to disintegration of the specimen: $c = 15\%$ and $t = 8$h.

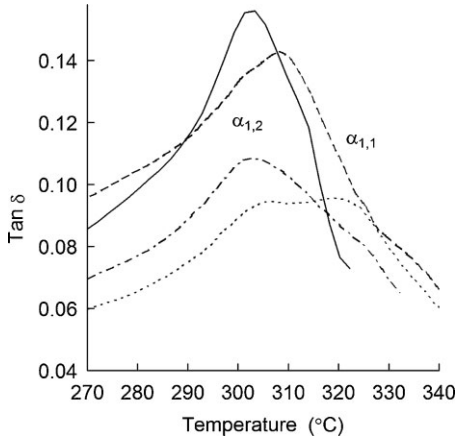

Figure 3.
DMA traces through the α_1 transition for composites prepared with $t = 8$ h, for $c = 5\%$ (solid line), 10% (dashes), 15% (dashes and dots), 20% (dots).

traces left the $\alpha_{1,1}$ peak on the high-temperature side.

Manabe et al. reported only one high temperature relaxation peak for α_1.[14] They studied samples of regenerated cellulose and found stronger damping for samples with very low crystallinity than for samples with moderate crystallinity. This observation provided the basis for the assignment of the α_1 transition to relaxation in non-crystalline regions. In the present work, we observed a similar dependence of $\alpha_{1,2}$ damping on crystallinity (Fig. 4). We therefore assign the $\alpha_{1,2}$ transition to relaxation in non-crystalline regions.

The $\alpha_{1,1}$ peak or shoulder was usually weaker than the $\alpha_{1,2}$ peak, making it difficult to obtain a meaningful measure of $\alpha_{1,1}$ damping. Visual comparisons between traces in Figs. 2 and 3 indicated that

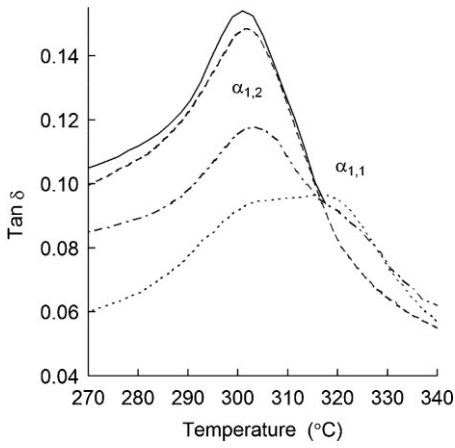

Figure 2.
DMA traces through the α_1 transition for composites prepared with $t = 1$ h and $c = 5\%$ (solid line), 10% (dashes), 15% (dashes and dots), 20% (dots).

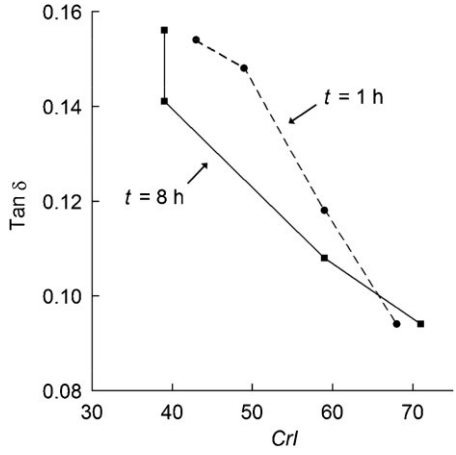

Figure 4.
Damping of $\alpha_{1,2}$ relaxation for composites with different crystallinity (*Crl*). Lines join points for composites prepared with $c = 5\%$, 10%, 15% and 20%, plotted from left to right.

$\alpha_{1,1}$ damping was strongest for the two composites with the highest values of *CrI*. Traces for those composites are shown as dotted lines in Figs. 2 and 3. Polymer chains within crystalline domains are likely to be too highly constrained to contribute to relaxation processes, so an assignment to polymer chain segments adjacent to crystalline domains seems more likely.

It is believed that the high temperature $\alpha_{1,1}$ peak was not observed in previous studies because the crystallinity of the cellulose materials was usually well below 50%.[14,16] This can only be completely resolved when the cellulosic material is highly crystalline ($CrI > 70\%$). Only all-cellulose composites can provide cellulose films with such a high crystallinity.

Duchemin et al. used X-ray diffraction and ^{13}C NMR spectroscopy to show that the crystalline domains in the cellulose composites were sometimes so small that the bulk of the cellulose chains are exposed to the surfaces of these domains.[23] The NMR data suggested that these surface chains accounted for between 16 wt.% and 28 wt.% of the samples used in the present work (*i.e.* $t = 8$ h). Similarly, there would be a corresponding mass of surface chains associated with the non-crystalline domains, no more than one chain width from the crystalline-non-crystalline boundary. Thus, in total the NMR data suggest that one third to one half of the total cellulose chain segments are associated with the crystalline-non-crystalline boundary. This provides an abundance of chain segments to contribute to $\alpha_{1,1}$ damping.

Chemical Decomposition

Cellulose pyrolysis begins at approximately 300°C.[28–30] The mechanisms for decomposition were reviewed, favouring a stepwise process starting with thermolytic cleavage of polymer chains in non-crystalline regions.[31] Further depolymerisation, ring-opening and cross-linking reactions lead to a mixture of char, tar and gases. Polymer chains in crystalline domains are relatively unreactive.[31] X-ray diffraction was used to characterise wood cellulose, demonstrating a decrease in the diameter of the cellulose microfibril during pyrolysis.[30] This observation suggests that the chemical decomposition begins with polymer chains exposed on the surfaces of crystalline domains, and proceeds by erosion into the interiors of those domains. This observation is also consistent with the thermogravimetry data provided by Ouajai *et al.* that explicitely shows that the matrix of regenerated cellulose is thermally less stable than the reinforcement that has a higher crystallinity.[32]

The $\alpha_{1,2}$ transition coincides with the onset of chemical decomposition. Depolymerisation of the polymer chains provides a possible mechanism for viscoelastic damping, in that the chain segments released by depolymerisation might participate in large-amplitude motions. Chains associated with the surfaces of crystalline domains would become involved at higher temperatures, releasing polymer segments to contribute to the $\alpha_{1,1}$ transition.

Chemical decomposition pathways include inter- and intra-chain cross-linking reactions that lead to char formation.[31] Such reactions help account for stiffening of some of the all-cellulose composites at temperatures above the $\alpha_{1,2}$ transition (Fig. 5 and 6).

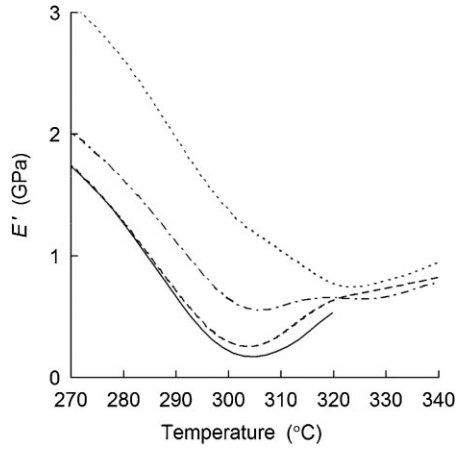

Figure 5.
Changes in the dynamic storage modulus *E'* through the α_1 transition for composites prepared with $t = 1$ h and $c = 5\%$ (solid line), 10% (dashes), 15% (dashes and dots), 20% (dots).

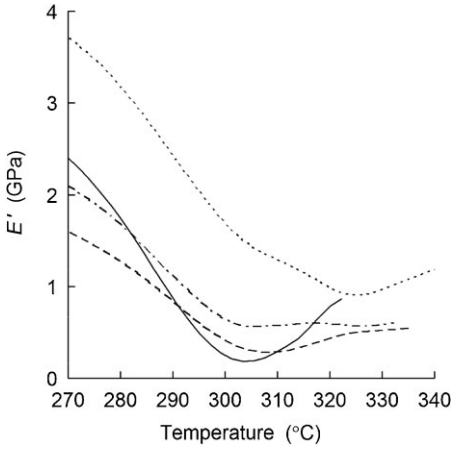

Figure 6.
Changes in the dynamic storage modulus *E'* through the α_1 transition for composites prepared with $t = 8$ h and $c = 5\%$ (solid line), 10% (dashes), 15% (dashes and dots), 20% (dots).

For the two all-cellulose composites with the lowest crystallinity, the dynamic storage modulus dropped to $E' = 0.2$ GPa at temperatures in the vicinity of 300°C to 310°C (Figs. 5 and 6). Both composites showed mechanical damage at approximately 320°C, ending the DMA experiments. The two composites with highest crystallinity did not soften to $E' < 0.8$ GPa before breaking at temperatures > 340°C. We attribute the better mechanical properties of the high-crystallinity composites to relatively thin non-crystalline domains between crystalline particles, so that most of the non-crystalline material was in close proximity to crystalline material and therefore relatively protected from depolymerisation.

Conclusion

DMA experiments on all-cellulose composites revealed two contributions to α_1 viscoelastic relaxation, assigned to segmental motion in non-crystalline polymer chains far from crystalline domains ($\alpha_{1,2}$ at 303 °C) or at boundaries between crystalline and non-crystalline domains ($\alpha_{1,1}$ at 325 °C). These temperatures are above the onset of chemical decomposition (300 °C), suggesting the involvement of products from partial depolymerisation of the polymer chains. High crystallinity is desirable for best mechanical performance at temperatures >300 °C.

Acknowledgements: The authors thank the Biopolymer Network Limited for funding under New Zealand Foundation for Research Science and Technology (BPLY0402). The authors also thank Mr. K. Stobbs for his help with mechanical testing and materials preparation and Mr. S. Brown for acquisition of the WAXD patterns. One of the authors (MPS) also acknowledges the support of the Brian Mason Scientific and Technical Trust.

[1] T. Nishino, K. Takano, K. Nakamae, *J Polym Sci, Part B: Polym Phys* **1995**, *33*, 1647.
[2] A. C. O'Sullivan, *Cellulose* **1997**, *4*, 173.
[3] M. Jarvis, *Nature* **2003**, *11*, 611.
[4] I. Sakurada, Y. Nukushina, T. Ito, *J Polym Sci* **1962**, *57*, 651.
[5] T. Nishino, I. Matsuda, K. Hirao, *Macromolecules* **2004**, *37*, 7683.
[6] W. Gindl, J. Keckes, *Polymer* **2005**, *46*, 10221.
[7] W. Gindl, T. Schoberl, J. Keckes, *Appl Phys A: Mater Sci Process* **2006**, *83*, 19.
[8] T. Nishino, N. Arimoto, *Biomacromolecules* **2007**, *8*, 2712.
[9] Q. Zhao, R. C. M. Yam, B. Zhang, Y. Yang, X. Cheng, R. K. Y. Li, *Cellulose* **2009**, *16*, 217.
[10] D. Porter, *Group Interaction Modelling of Polymer Properties*;, CRC Press, New York **1995**.
[11] L. Szcześniak, A. Rachocki, J. Tritt-Goc, *Cellulose* **2008**, *15*, 445.
[12] N. L. Salmén, E. L. Back, *Tappi J.* **1977**, *60*, 137.
[13] E. Vittadini, L. C. Dickinson, P. Chinachoti, *Carbohydr Polym* **2001**, *46*, 49.
[14] S. Manabe, M. Iwata, K. Kamide, *Polym J* **1986**, *18*, 1.
[15] S. A. Bradley, H. Carr, *J Polym Sci, Part B: Polym Phys* **1976**, *14*, 111.
[16] T. Hongo, C. Yamane, M. Saito, K. Okajima, *Polym J* **1996**, *28*, 769.
[17] C. Yamane, M. Mori, M. Saito, K. Okajima, *Polym J* **1996**, *28*, 1039.
[18] S. Yano, H. Hatakeyama, T. Hatakeyama, *J Appl Polym Sci* **1976**, *20*, 3221.
[19] T. Kondo, C. Sawatari, *Polymer* **1996**, *37*, 393.
[20] P. Langan, Y. Nishiyama, H. Chanzy, *J Am Chem Soc* **1999**, *121*, 9940.
[21] Y. Nishiyama, P. Langan, H. Chanzy, *J Am Chem Soc* **2002**, *124*, 9074.
[22] Y. Nishiyama, J. Sugiyama, H. Chanzy, P. Langan, *J Am Chem Soc* **2003**, *125*, 14300.

[23] B. Duchemin, R. Newman, M. Staiger, *Cellulose* **2007**, *14*, 311.
[24] E. Bianchi, A. Ciferri, G. Conio, A. Cosani, M. Terbojevich, *Macromolecules* **1985**, *18*, 646.
[25] L. Segal, J. J. Creely, A. E. Martin, C. M. Conrad, *Text Res J* **1959**, *29*, 786.
[26] B. J. C. Duchemin, R. H. Newman, M. P. Staiger, *Compos Sci Tech* **2009**, *69*, 1225.
[27] G. Conio, P. Corazza, E. Bianchi, A. Tealdi, A. Ciferri, *J Polym Sci, Part C: Polym Lett* **1984**, *22*, 273.
[28] M. Essig, G. N. Richards, E. Schenck, In: *Mechanisms of formation of the major volatile products from the pyrolysis of cellulose*, C. Schuerch, Ed., John Wiley and Sons, Syracuse **1989**, 841.
[29] H. Yang, R. Yan, H. Chen, D. H. Lee, C. Zheng, *Fuel* **2007**, *86*, 1781.
[30] G. A. Zickler, W. Wagermaier, S. S. Funari, M. Burghammer, O. J. Paris, *Anal Appl Pyrolysis* **2007**, *80*, 134.
[31] R. Ball, A. C. McIntosh, J. Brindley, *Phys Chem Chem Phys* **1999**, *1*, 5035.
[32] S. Ouajai, R. A. Shanks, *Composites Science and Technology* **2009**, *69*, 2119.

